

Impacts of hydrogen annealing on the carrier lifetimes in p-type 4H-SiC after thermal oxidation

Ruijun Zhang(张锐军), Rongdun Hong(洪荣墩), Jingrui Han(韩景瑞), Hungkit Ting(丁雄杰), Xiguang Li(李锡光), Jiafa Cai(蔡加法), Xiaping Chen(陈厦平), Deyi Fu(傅德颐), Dingqu Lin(林鼎渠), Mingkun Zhang(张明昆), Shaoxiong Wu(吴少雄), Yuning Zhang(张宇宁), Zhengyun Wu(吴正云), and Feng Zhang(张峰)

Citation: Chin. Phys. B, 2023, 32 (**6**): 067205. DOI: 10.1088/1674-1056/ac89db
Journal homepage: http://cpb.iphy.ac.cn; http://iopscience.iop.org/cpb

What follows is a list of articles you may be interested in

Ultra-high voltage 4H-SiC gate turn-off thyristor forlow switching time

Qing Liu(刘青), Hong-Bin Pu(蒲红斌), Xi Wang(王曦)
Chin. Phys. B, 2019, 28 (**12**): 127201. DOI: 10.1088/1674-1056/ab4e89

Numerical and experimental study of the mesa configuration in high-voltage 4H-SiC PiN rectifiers

Xiao-Chuan Deng(邓小川), Xi-Xi Chen(陈茜茜), Cheng-Zhan Li(李诚瞻), Hua-Jun Shen(申华军), Jin-Ping Zhang(张金平)
Chin. Phys. B, 2016, 25 (**8**): 087201. DOI: 10.1088/1674-1056/25/8/087201

Design consideration and fabrication of 1.2-kV 4H-SiC trenched-and-implanted vertical junction field-effect transistors

Chen Si-Zhe (陈思哲), Sheng Kuang (盛况)
Chin. Phys. B, 2014, 23 (**7**): 077201. DOI: 10.1088/1674-1056/23/7/077201

Experimental and numerical analyses of high voltage 4H-SiC junction barrier Schottky rectifiers with linearly graded field limiting ring

Wang Xiang-Dong (王向东), Deng Xiao-Chuan (邓小川), Wang Yong-Wei (王永维), Wang Yong (王勇), Wen Yi (文译), Zhang Bo (张波)
Chin. Phys. B, 2014, 23 (**5**): 057203. DOI: 10.1088/1674-1056/23/5/057203

A novel 4H-SiC lateral bipolar junction transistor structure with high voltage and high current gain

Deng Yong-Hui (邓永辉), Xie Gang (谢刚), Wang Tao (汪涛), Sheng Kuang (盛况)
Chin. Phys. B, 2013, 22 (**9**): 097201. DOI: 10.1088/1674-1056/22/9/097201

SPECIAL TOPIC — Celebrating the 100th Anniversary of Physics Discipline of Xiamen University

Impacts of hydrogen annealing on the carrier lifetimes in p-type 4H-SiC after thermal oxidation

Ruijun Zhang(张锐军)[1], Rongdun Hong(洪荣墩)[1,†], Jingrui Han(韩景瑞)[2], Hungkit Ting(丁雄杰)[2], Xiguang Li(李锡光)[2], Jiafa Cai(蔡加法)[1], Xiaping Chen(陈厦平)[1], Deyi Fu(傅德颐)[1], Dingqu Lin(林鼎渠)[1], Mingkun Zhang(张明昆)[1], Shaoxiong Wu(吴少雄)[1], Yuning Zhang(张宇宁)[1], Zhengyun Wu(吴正云)[1], and Feng Zhang(张峰)[1,‡]

[1] *Department of physics, Xiamen university, Xiamen* 361005, *China*
[2] *Guangdong Tianyu Semiconductor Co., Ltd, Dongguan* 523808, *China*

(Received 1 July 2022; revised manuscript received 8 August 2022; accepted manuscript online 16 August 2022)

Thermal oxidation and hydrogen annealing were applied on a 100 μm thick Al-doped p-type 4H-SiC epitaxial wafer to modulate the minority carrier lifetime, which was investigated by microwave photoconductive decay (μ-PCD). The minority carrier lifetime decreased after each thermal oxidation. On the contrary, with the hydrogen annealing time increasing to 3 hours, the minority carrier lifetime increased from 1.1 μs (as-grown) to 3.14 μs and then saturated after the annealing time reached 4 hours. The increase of surface roughness from 0.236 nm to 0.316 nm may also be one of the reasons for limiting the further improvement of the minority carrier lifetimes. Moreover, the whole wafer mappings of minority carrier lifetimes before and after hydrogen annealing were measured and discussed. The average minority carrier lifetime was up to 1.94 μs and non-uniformity of carrier lifetime reached 38% after 4-hour hydrogen annealing. The increasing minority carrier lifetimes could be attributed to the double mechanisms of excess carbon atoms diffusion caused by selective etching of Si atoms and passivation of deep-level defects by hydrogen atoms.

Keywords: 4H-SiC, carrier lifetime, hydrogen annealing

PACS: 72.20.Jv, 72.80.Jc **DOI:** 10.1088/1674-1056/ac89db

1. Introduction

Silicon carbide (SiC) has received increasing attention as a significant semiconductor material for ultrahigh-voltage and low-loss power devices owing to its superior physical properties such as wide band gap (3.26 eV), high carrier saturation rate (1200 $cm^2 \cdot V^{-1} \cdot s^{-1}$) and good thermal conductivity (4.9 $W \cdot cm^{-1} \cdot K^{-1}$).[1,2] The bipolar devices require a long carrier lifetime to achieve sufficient conductivity modulation in the forward conduction mode.[3] The carrier lifetime usually observed in 4H-SiC epilayer is approximately less than 1 μs after growth, which is not adequate to promote the conductivity modulation of 4H-SiC for ultra-high voltage application. Therefore, it is significant to improve the carrier lifetime in 4H-SiC epilayer. The trap centers depressing the minority carrier lifetime in n-type 4H-SiC epilayer have been reported by several groups.[4–6] At present, the major carrier lifetime killer for n-type 4H-SiC is well known as the $Z_{1/2}$ center,[7,8] which is considered to be the defect center related to carbon vacancies (V_C). The density of the $Z_{1/2}$ center in SiC epitaxial layers is strongly dependent on the growth conditions.[9] On the one hand, it is achievable to reduce the density of the $Z_{1/2}$ by optimizing the C/Si ratio and the growth temperature during the expitaxy growth.[10] On the other hand, the $Z_{1/2}$ defect centers can be eliminated and very long minority carrier lifetimes of 20–30 μs in n-type 4H-SiC epilayer have been obtained by high temperature oxidation or carbon ion implantation after post-processing.[11–13] However, the same methods being applied to p-type 4H-SiC epilayer do not work well,[14] which makes it difficult to improve the carrier lifetimes of p-type 4H-SiC.[15,16] In p-type SiC, the $EH_{6/7}$ center rather than the $Z_{1/2}$ center must be more involved in the carrier recombination.[17] Takafumi Okuda *et al.* reported an improvement of minority carrier lifetimes in p-type 4H-SiC epilayers by hydrogen annealing.[18] But the mechanism of hydrogen annealing is still unclear.

In this study, the minority carrier lifetimes in 100 μm thick p-type 4H-SiC epilayer after 1300 °C thermal oxidation and different cumulative hydrogen annealing time were measured by microwave photoconductive decay (μ-PCD). Furthermore, the mechanisms of hydrogen annealing effects on the minority carrier lifetimes have been studied and demonstrated by analysis of photoluminescence images and the surface roughness after long-time hydrogen annealing.

†Corresponding author. E-mail: rdhong@xmu.edu.cn
‡Corresponding author. E-mail: fzhang@xmu.edu.cn

© 2023 Chinese Physical Society and IOP Publishing Ltd

2. Experiment

The samples used in this study were Al-doped p-type 4H-SiC epitaxial wafer homoepitaxially grown on 4° off-axis (0001) substrates by chemical vapor deposition. The thickness was 100 μm and the doping concentration was 2×10^{14} cm^{-3}. The sample was thermally oxidized at 1300 °C for 5 h (1st thermal oxidation) after standard RCA cleaning and applied on segmented annealing in hydrogen at 1000 °C under low pressure, with cumulative annealing time of 1 h, 1.5 h, 2 h, 3 h and 4 h respectively (1st hydrogen annealing), by using the LPE-1O9 equipment. After 4 h hydrogen annealing, the sample was thermally oxidized again at 1300 °C for 8 h (2nd thermal oxidation) and annealed in hydrogen again at 1000 °C for 0.5 h and 1 h (2nd hydrogen annealing), which was followed by the 3rd thermal oxidation for 16 h. The 3rd hydrogen annealing was carried out at 1000 °C for 1 h after the 3rd thermal oxidation. The above three times thermal oxidation and three times hydrogen annealing were used in order to further verify the decrease of minority carrier lifetime after oxidation and the increase of minority carrier lifetime after hydrogen annealing. The oxidation time increased from 5 h to 16 h in order to rule out the insufficient oxidation time as the cause of minority carrier lifetime decrease.

Table 1. Process parameters and minority carrier lifetime.

Process	Annealing temperature (°C)	Annealing time (h)	Carrier lifetime (μs)
As-grown			1.65
1st thermal oxidation	1300	5	1.10
1st hydrogen annealing	1000	4	2.99
2nd thermal oxidation	1300	8	1.28
2nd hydrogen annealing	1000	1	1.94
3rd thermal oxidation	1300	16	1.12
3rd hydrogen annealing	1000	2	2.81

The curves of photoconductivity decay and the whole wafer mappings of minority carrier lifetimes were measured by μ-PCD measurement of Semilabs WT-2000 instrument at room temperature. In the μ-PCD measurement, the samples were excited by an yttrium lithium fluoride (YLF) laser with a 349 nm wavelength and a 15 ns pulse width. During measurements, the decay of the photoconductivity which indicated the variation of excess carrier concentration was monitored by microwave reflectivity at a frequency of 26 GHz. And, photoluminescence (PL) excited by laser with 313 nm wavelength was employed to study the original state and the change of sample defects after the thermal oxidation. At last, the surface roughness was measured by atomic force microscopy (AFM).

3. Results and discussion

3.1. Thermal oxidation

Figure 1 shows the normalized photoconductivity decay curves of the 100 μm thick Al-doped p-type 4H-SiC epilayers as-grown and after the post-treatment. It is worth noting that the minority carrier lifetime of the sample decreased from 1.65 μs to 1.10 μs after the 1st thermal oxidation at 1300 °C for 5 h. On the contrary, after the 1st hydrogen annealing at 1000 °C for 4 h, the minority carrier lifetime increased from 1.10 μs to 2.99 μs, which will be discussed in detail in the next section. While the 2nd thermal oxidation at 1300 °C for 8 h was carried out on the sample, the same decrease of minority carrier lifetime as that after the 1st thermal oxidation was observed.

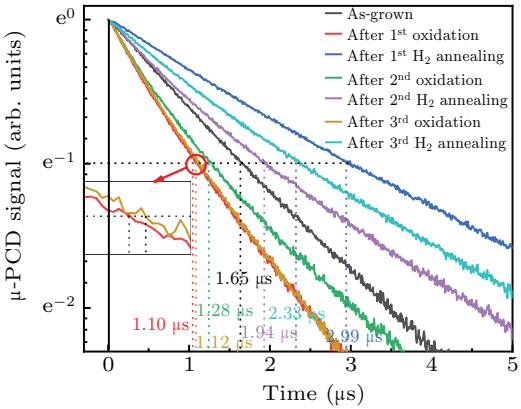


Fig. 1. The μ-PCD decay curves at room temperature are obtained from a 100 μm thick p-type 4H-SiC epilayer. The decay curves of as-grown epilayer as well as before-and-after three-times thermal oxidation at 1300 °C are demonstrated.

Likewise, the increase and decrease of the minority carrier lifetime were respectively observed after the 2nd hydrogen annealing at 1000 °C for 1 h and the 3rd thermal oxidation 1300 °C for 16 h. With the increase of the thermal oxidation time, the minority carrier lifetime did not decrease significantly further, which was because the excess carbon atoms introduced by thermal oxidation eliminated the role of carbon vacancy and hydrogen annealing.

The decrease of the minority carrier lifetime after thermal oxidation was also reported in Takafumi Okuda's study.[19] Although it was reported that the elimination of the $Z_{1/2}$ center by the thermal oxidation would enhance the minority carrier lifetime of the N-type SiC epitaxial layer,[20] the elimination of the $Z_{1/2}$ center in the p-type SiC epitaxial layer would be very limited after the thermal oxidation.[21] The reason of the carrier lifetime decrease is considered as follows. On the one hand, the benefit of the elimination of the $Z_{1/2}$ center by thermal oxidation may be cancelled by generating another deep level by the oxidation, such as the HK0 center,[22] and that the thermal oxidation may also eliminate partially hydrogen passivation in this process. On the other hand, the oxidation degree of the SiC area with dislocations and stacking faults would be higher than that without dislocation and stacking faults, and surface pits would form base on the dislocations and stacking faults after oxidation.[23,24] Those surface pits could fur-

ther enhance the carrier recombination and reduce the carrier lifetime.[25] The PL images are shown in Fig. 2, which illustrates the change of the original state and the change of sample defects after each thermal oxidation. The outcrops of surface pits became larger and more obvious after each thermal oxidation. Therefore, the 1300 °C thermal oxidation might enhance the surface recombination of SiC epitaxial wafers and decrease the minority carrier lifetime.

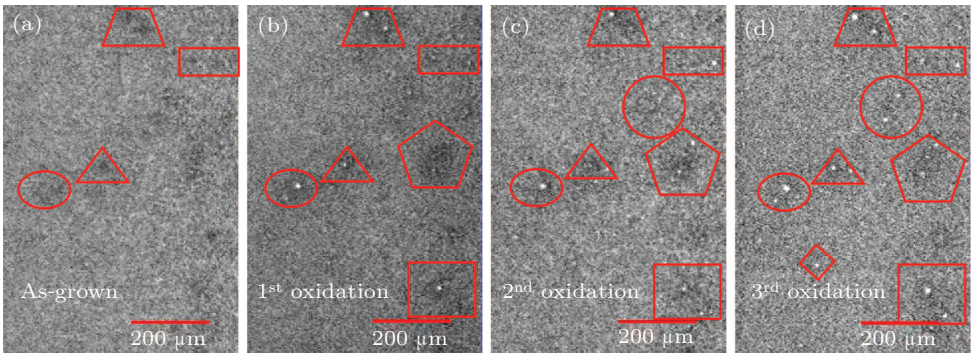


Fig. 2. PL images of the 4H-SiC epilayer: (a) as-grown and (b), (c), (d) after thermal oxidation at 1300 °C for 5 h, 8 h, 16 h.

3.2. Hydrogen annealing

After the 1st oxidation, the 100 μm thick Al-doped p-type SiC epilayers ($N_A = 2 \times 10^{14}$ cm^{-3}) were annealed in hydrogen atmosphere for 4 h, and the μ-PCD photoconductivity decay curves at different cumulative annealing time are illustrated and studied in Fig. 3(a). After the cumulative annealing time reached 1 h, the minority carrier lifetimes increased from 1.10 μs to 2.00 μs and then increased to 2.74 μs after the cumulative annealing time reached 2 h. Another hour later, the minority carrier lifetimes increased to 3.14 μs. When the cumulative annealing time reached 4 h, a slight decrease of the minority carrier lifetimes was observed. It could be concluded that the minority carrier lifetimes increased with the cumulative annealing time, and saturated after the cumulative annealing reached 3 h. In the same way, the second hydrogen annealing was carried for 1 h (0.5 h×2) after the 2nd oxidation, and the third hydrogen annealing was carried for 2 h after the 3rd oxidation. As shown in Figs. 3(b) and 3(c), the minority carrier lifetime of the sample was also increased with cumulative annealing time.

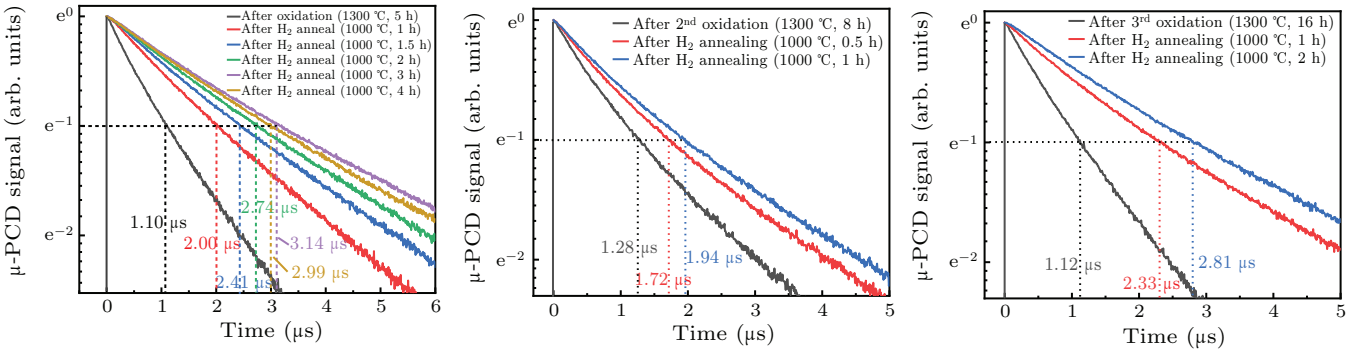


Fig. 3. Photoconductivity decay curves measured for a 100 μm Al-doped p-type 4H-SiC epilayer ($N_A = 2 \times 10^{14}$ cm^{-3}) at RT. (a) Decay curves are shown for the first H_2-annealed 1–4 h samples. (b) Decay curves are shown for the second H_2-annealed 0.5 h and 1 h samples. (c) Decay curves are shown for the third H_2-annealed 1 h and 2 h samples.

As shown in Fig. 4, the surface roughness after the 1st hydrogen annealing was also measured and it was found that there was no significant change until the cumulative annealing time reached 3 h. After then, the surface roughness began to increase. When the cumulative annealing time reached 4 h, the surface roughness increased to 0.316 nm and the minority carrier lifetime also decreased from 3.14 μs to 2.99 μs. The large variation of surface roughness might increase the surface recombination which could limit the minority carrier lifetimes and result in the slight decrease of the minority carrier lifetime of the sample after 4 h cumulative annealing.[26,27] There was almost no change on surface roughness within a short-time hydrogen annealing (2nd and 3rd hydrogen annealings).

The interreaction between hydrogen atoms and silicon carbide during the annealing process is quite complex,[28,29] which could generate Si–H, C–H,[30] Al–H complex,[31] and V_C–H complex.[32] The effects of 10–20 min hydrogen annealing on increasing the minority carrier lifetimes were basically independent of the annealing time, according to OKUDA who stated that the unknown deep level defects were passivated by hydrogen atoms in p-type SiC epilayers during hydrogen annealing.[33] Due to the small radius of hydrogen atoms

and their tendency to diffuse in silicon carbide at relative low temperature of 1000 °C, hydrogen passivation of deep level defects was supposed to be accomplished in a short time (10–20 min). In our study, under the condition of low pressure and long time (several hours) hydrogen annealing, the minority carrier lifetimes further increased, which is mainly attributed to selective etching rather than the hydrogen passivation of deep level defects. The mechanism of selective etching can be depicted by the following chemical equations:

$$\mathrm{Si(s)} \rightarrow \mathrm{Si(g)}, \tag{1}$$

$$\mathrm{C(s)} + 2\mathrm{H_2} \rightarrow \mathrm{CH_4(g)}, \tag{2}$$

where "g" and "s" represent the gas and solid phases of the reactive matter during the annealing process. In chemical reactions involving gas molecules, the equilibrium tends to produce more gas molecules when the pressure is lowered. Therefore, it can be deduced from Eqs. (1) and (2) that hydrogen annealing under low pressure will produce a selective etching,[34,35] which can enhance the desorption of Si atoms and inhibit the etching of carbon atoms. The desorption of silicon atoms on the surface may lead to the formation of some extra carbon atoms, and the long-time hydrogen annealing may result in the diffusion of carbon atoms into the epilayer bulk, thus eliminating a part of V_C defects. This may be the reason for the further increase of the minority carrier lifetimes. In addition, a small number of extra carbon atoms introduced by thermal oxidation would diffuse further and eliminate carbon vacancy relevant defects, which could further improve the minority carrier lifetime. This may be the reason why the minority carrier lifetime of the third hydrogen annealing was longer than that of the second hydrogen annealing with the same annealing time.

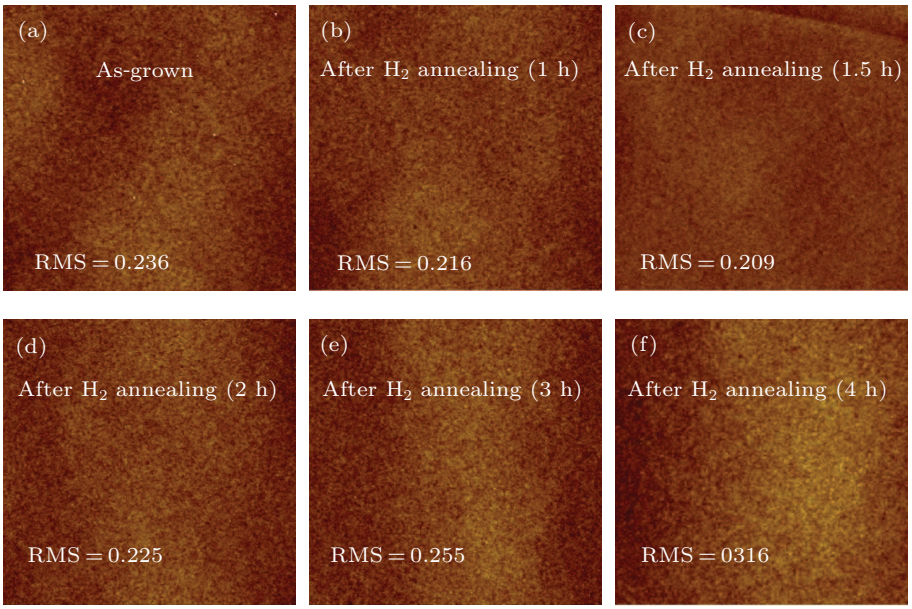


Fig. 4. Surface roughness measured for a 100 μm thick Al-doped p-type 4H-SiC epilayer ($N_A = 2 \times 10^{14}$ cm^{-3}) by AFM. RMS are shown for the as-grown, H_2-annealed 1–4 h samples.

Figures 5(a)–5(f) show the mappings of minority carrier lifetimes of the sample with different cumulative annealing times. The non-uniformity of minority carrier lifetimes was calculated by the following equation:

$$\bar{X} = \frac{1}{N}\sum_{i=1}^{N} X_i, \tag{3}$$

$$\mathrm{Std} = \sqrt{\frac{1}{N-1}\sum_{i=1}^{N}(X_i - \bar{X})^2}, \tag{4}$$

$$\mathrm{Nonuni.} = 1 - \frac{\mathrm{Std}}{\bar{X}}. \tag{5}$$

It was worth noting that with the increase of the cumulative annealing time, the average minority carrier lifetimes as well as the non-uniformity of minority carrier lifetimes increased, indicating that the crystal quality of the epilayer had a great influence on the minority carrier lifetimes. As shown in Figs. 5(a)–5(f), the increase of minority carrier lifetime of SiC epitaxial wafer was mainly manifested in the position marked by the circle. The average minority carrier lifetime at the position of the red circle in Figs. 5(a) and 5(e) was 1.47 μs and 2.96 μs, respectively, indicating that the minority carrier lifetime at other locations did not increase significantly. Due to the rotation of the tray during hydrogen annealing, the non-uniformity caused by hydrogen annealing was excluded. The main problem lied in the epilayer growth and defects. There existed the deep-level defects in the epilayer outside the circle marked which could not be passivated by hydrogen atoms and could restricted the increase of the minority carrier lifetimes. Therefore, there was no significant minority carrier lifetime increase in these locations of epilayers when the average minority carrier lifetime was increasing. The defects which cannot

be passivated by hydrogen are called DNPH (defects that are not passivated by hydrogen). The minority carrier lifetimes could be improved obviously at the position with low DNPH concentration, but it was difficult to improve the minority carrier lifetimes at the position with high DNPH concentration. This was the reason why the non-uniformity of minority carrier lifetimes increased with the increase of minority carrier lifetimes.

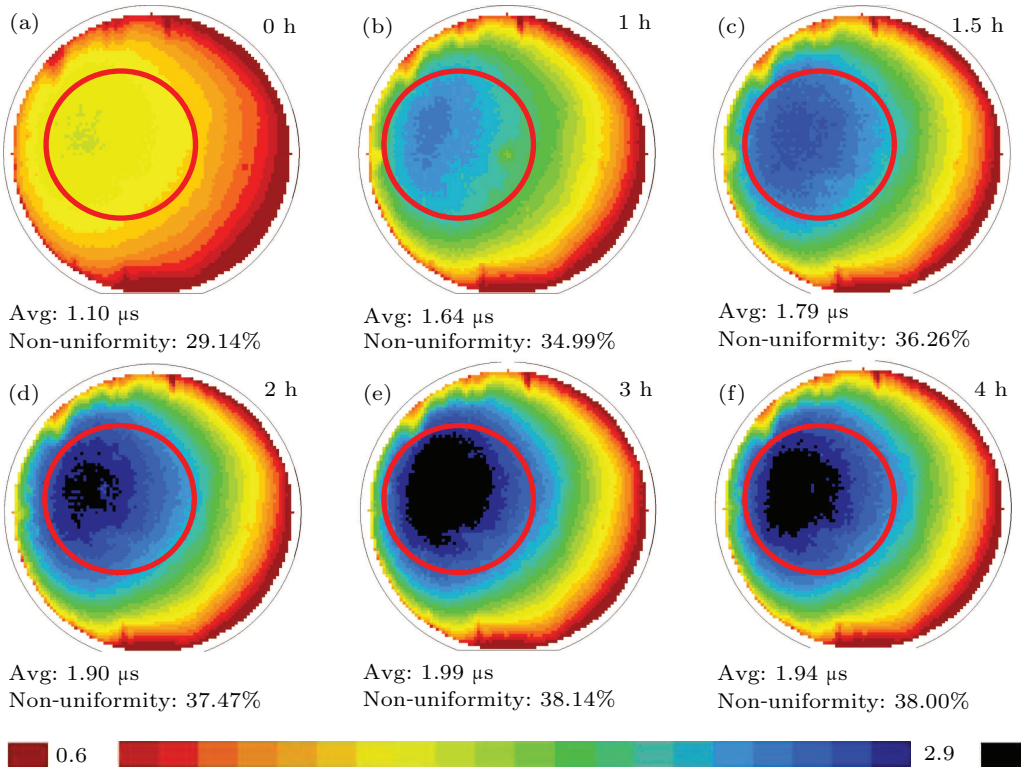


Fig. 5. Minority carrier lifetime mapping over 4 inch wafer measured by μ-PCD with 1 mm lateral step size and non-uniformity was calculated: (a) the as-grown, (b)–(f) after H_2-annealed at 1–4 h.

4. Conclusion

During the fabrication of SiC devices, the fabrication of oxide layers was usually accomplished by thermal oxidation at 1000–1300 °C. It takes longer to eliminate V_C defects in this temperature range. But if the epilayer contains a lot of surface defects, then a short period of low temperature oxidation could lead to more serious surface recombination, resulting in a decrease in minority carrier lifetime. This indicates that the epilayer quality during the fabrication of the oxide layer would play an important role in most 4H-SiC electron devices. The relation between the minority carrier lifetime and hydrogen annealing was studied to offset the decrease of minority carrier lifetime caused by the thermal oxidation process and improve the minority carrier lifetime as long as possible. The epitaxial wafer after thermal oxidation was annealed in hydrogen under low pressure for a long time and it was observed that the minority carrier lifetimes increased with the increase of the cumulative annealing time. When the cumulative annealing time reached 3 h, the minority carrier lifetimes reached 3.14 μs and then remained basically unchanged. The increasing minority carrier lifetimes could be attributed to the double mechanisms of excess carbon atoms diffusion caused by selective etching of Si atoms during hydrogen annealing to eliminate carbon vacancies and passivation of deep-level defects by hydrogen atoms. With the increase of minority carrier lifetimes in hydrogen annealing, the non-uniformity of minority carrier lifetimes as well as the surface roughness also increased, which might be the reason that the minority carrier lifetimes could not be further improved.

Acknowledgements

Project supported by Key Area Research and Development Project of Guangdong Province, China (Grant No. 2020B010170002), the Science Challenge Project (Grant No. TZ2018003-1-101), the Natural Science Foundation of Fujian Province of China for Distinguished Young Scholars (Grant No. 2020J06002), the Science and Technology Project of Fujian Province of China (Grant No. 2020I0001), the Fundamental Research Funds for the Central Universities (Grant Nos. 20720190049 and 20720190053), and the Science and Technology Key Projects of Xiamen (Grant No. 3502ZCQ20191001), and the National Natural Science Foundation of China (Grant No. 51871189).

References

[1] Matsunami H and Kimoto T 1997 *Materials Science & Engineering R-Reports* **20** 125

[2] Cooper J A, Melloch M R, Singh R, Agarwal A and Palmour J W 2002 *Ieee Transactions on Electron Devices* **49** 658

[3] Kimoto T, Yamada K, Niwa H and Suda J 2016 *Energies* **9** 908

[4] Zhang J, Storasta L, Bergman J P, Son N T and Janzen E 2003 *J. Appl. Phys.* **93** 4708

[5] Tawara T, Tsuchida H, Izumi S, Kamata I and Izumi K 2004 *Silicon Carbide and Related Materials 2003, Prts 1 and 2*, Madar R and Camassel J eds. pp. 565–568

[6] Danno K, Nakamura D and Kimoto T 2007 *Appl. Phys. Lett.* **90** 202109

[7] Klein P B, Shanabrook B V, Huh S W, Polyakov A Y, Skowronski M, Sumakeris J J and O'Loughlin M J 2006 *Appl. Phys. Lett.* **88** 052110

[8] Beyer F C, Hemmingsson C G, Pedersen H, Henry A, Isoya J, Morishita N, Ohshima T and Janzen E 2012 *J. Phys. D-Appl. Phys.* **45** 455301

[9] Kimoto T, Nakazawa S, Hashimoto K and Matsunami H 2001 *Appl. Phys. Lett.* **79** 2761

[10] Kimoto T, Hashimoto K and Matsunami H 2003 *Jpn. J. Appl. Phys.* **42** 7294

[11] Storasta L and Tsuchida H 2007 *Appl. Phys. Lett.* **90** 062116

[12] Hiyoshi T and Kimoto T 2009 *Appl. Phys. Express* **2** 041101

[13] Miyazawa T, Ito M and Tsuchida H 2010 *Appl. Phys. Lett.* **97** 202106

[14] Hayashi T, Asano K, Suda J and Kimoto T 2012 *J. Appl. Phys.* **112** 064503

[15] Liaugaudas G, Dargis D, Kwasnicki P, Arvinte R, Zielinski M and Jarasiunas K 2015 *J. Phys. D-Appl. Phys.* **48** 025103

[16] Zhang R J, Hong R D, Cai J F, Chen X P, Lin D Q, Zhang M K, Wu S X, Zhang Y N, Han J R, Wu Z Y and Zhang F 2021 *IEEE Workshop on Wide Bandgap Power Devices and Applications in Asia*, WiPDA Asia 2021, August 25, 2021–August 27, 2021, Wuhan, China, pp. 281–284

[17] Kimoto T, Niwa H, Okuda T, Saito E, Zhao Y, Asada S and Suda J 2018 *J. Phys. D-Appl. Phys.* **51** 363001

[18] Okuda T, Miyazawa T, Tsuchida H, Kimoto T and Suda J 2014 *Appl. Phys. Express* **7** 085501

[19] Okuda T, Kimoto T and Suda J 2013 *Appl. Phys. Express* **6** 121301

[20] Ichikawa S, Kawahara K, Suda J and Kimoto T 2012 *Appl. Phys. Express* **5** 101301

[21] Hayashi T, Asano K, Suda J and Kimoto T 2011 *J. Appl. Phys.* **109** 014505

[22] Danno K and Kimoto T 2007 *J. Appl. Phys.* **101** 103704

[23] Powell J A, Petit J B, Edgar J H, Jenkins I G, Matus L G, Choyke W J, Clemen L, Yoganathan M, Yang J W and Pirouz P 1991 *Appl. Phys. Lett.* **59** 183

[24] Nakano Y, Nakamura T, Kamisawa A and Takasu H 2009 *International Conference on Silicon Carbide and Related Materials*, 2009,Oct 14–19, Otsu, JAPAN, pp. 377–380

[25] Kimoto T, Hiyoshi T, Hayashi T and Suda J 2010 *J. Appl. Phys.* **108** 083721

[26] Klein P B 2008 *J. Appl. Phys.* **103** 033702

[27] Mori Y, Kato M and Ichimura M 2014 *J. Phys. D-Appl. Phys.* **47** 335102

[28] Deak P, Gali A and Aradi B 2001 *Silicon Carbide and Related Materials, Ecscrm2000*, Pensl G, *et al*. eds. pp. 421–426

[29] Yan G G, Zhang F, Niu Y X, Yang F, Liu X F, Wang L, Zhao W S, Sun G S and Zeng Y P 2015 *Appl. Surf. Sci.* **353** 744

[30] Tsuchida H, Kamata I and Izumi K 1997 *Appl. Phys. Lett.* **70** 3072

[31] Samiji M E, Venter A, Wagener M C and Leitch A W R 2001 *J. Phys.-Condens. Matter* **13** 9011

[32] Gali A, Aradi B, Deak P, Choyke W J and Son N T 2000 *Phys. Rev. Lett.* **84** 4926

[33] Okuda T, Miyazawa T, Tsuchida H, Kimoto T and Suda J 2017 *J. Electron. Mater.* **46** 6411

[34] Charrier A, Coati A, Argunova T, Thibaudau F, Garreau Y, Pinchaux R, Forbeaux I, Debever J M, Sauvage-Simkin M and Themlin J M 2002 *J. Appl. Phys.* **92** 2479

[35] Sun C Z, Cai W W, Hong R D, Wu J K, Chen X P, Cai J F, Zhang F and Wu Z Y 2020 *Journal of Physics and Chemistry of Solids* **137** 109224